Title
Heat Treatment Optimizations for Wind-and-React Bi-2212 Racetrack Coils

Authors
Godeke, A
Cheng, DW
Dietderich, DR
et al.

Publication Date
2012

DOI
10.1016/j.phpro.2012.06.047

Peer reviewed

Available online at www.sciencedirect.com

SciVerse ScienceDirect

Physics Procedia 36 (2012) 812 – 817

Physics Procedia

Superconductivity Centennial Conference

Heat treatment optimizations for Wind-and-React Bi-2212 racetrack coils

A. Godeke, D. W. Cheng, D. R. Dietderich, M. G. T. Mentink, S. O. Prestemon, G. L. Sabbi

Lawrence Berkeley National Laboratory, 1 Cyclotron Rd., Berkeley, CA 94720, USA

Abstract

Lawrence Berkeley National Laboratory (LBNL) is developing Wind-and-React (W&R) $Bi_2Sr_2CaCu_2O_{8+\delta}$ (Bi-2212) accelerator magnet technology for insert coils, to surpass the intrinsic limitations of Nb-based magnets, and eventually develop hybrid systems that can approach 20 T dipole fields. The Bi-2212 technology is being developed in close collaboration with industry, and has been partly supported by the US Very High Field Superconducting Magnet Collaboration (VHFSMC). Steady improvements were made over the last several years, with coil HTS-SC08 reaching 2636 A, or about 85% of its witness sample critical current (I_c). Though this is still a factor 3 to 4 too low to be competitive with Nb-based materials, it is expected that the required I_c can be achieved through further conductor optimizations. Recent developments include the commissioning of infrastructure for the reaction of coils at LBNL. Earlier coils were fabricated and tested at LBNL, but were reacted at the wire manufacturer. We describe in detail the furnace calibrations and heat treatment optimizations that enable coil reactions at temperatures approaching 890 °C with a homogeneity of ±1 °C in a pure oxygen flow. We reacted two new coils at LBNL, and tested the performance of coil HTS-SC10 at 4.2 K in self-field using a superconducting transformer system. We find that its performance is consistent with witness samples, and comparable to coil HTS-SC08, which is an identical coil that was reacted at Oxford Instruments Superconductor Technology (OST), thereby validating the in-house reaction process.

Keywords: Keywords: Bi-2212, $Bi_2Sr_2CaCu_2O_{8+\delta}$, accelerator magnet, superconducting magnet, heat treatment

1. Introduction

The performance of high field superconducting dipole magnets, constructed of Nb-based superconducting materials, is intrinsically limited to 10.5 T at 1.9 K for NbTi, and to 18 T at 1.9 K for Nb_3Sn [1]. NbTi dipoles are limited due to the available upper critical magnetic field as a function of temperature ($H_{c2}(T)$), whereas Nb_3Sn dipoles are limited due to insufficient pinning efficiency at high magnetic fields. There are two possible routes to progress beyond the present superconducting dipole record field of 16 T [2]. The first is by creating approximately a factor 10 refinement of the pinning structures in Nb_3Sn through grain refinement or the introduction of engineered pinning centers, which has the potential to increase the Nb_3Sn dipole limit to about 20 T at 4.2 K or 22 T at 1.9 K [1]. Though successful on thin films [3, 4], it is at present unknown how to achieve this in wires, even though initial attempts have been made [5, 6]. A second route is to switch to a material that has a higher H_{c2}. Among the candidate materials Bi-2212 is the most advanced, since it is available as a round wire and generally compatible with established approaches to accelerator

1875-3892 doi:10.1016/j.phpro.2012.06.047

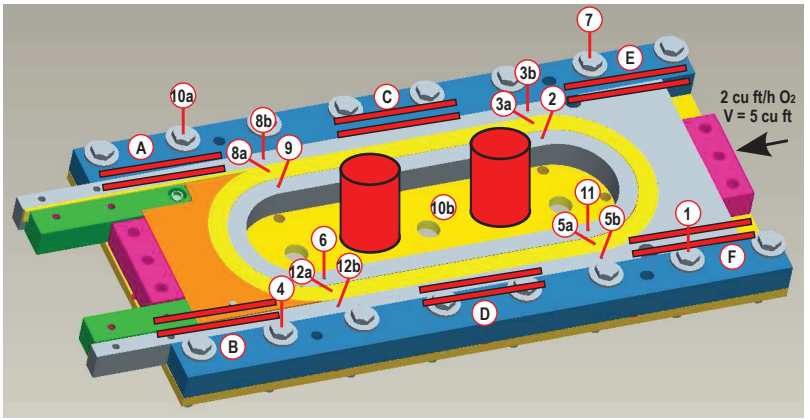

Fig. 1. Schematic representation of an instrumented HTS sub-scale coil. Numbers 1–12 depict thermocouple locations, and letters A–F depict the locations of short straight witness samples. The central cylindrical elements represent helical witness samples on holders.

coil fabrication [7]. Its wire, or engineering, current density J_E is presently a factor 3 – 4 too low to be competitive with Nb_3Sn, but the recent discovery of bubbles as a main current blocking mechanism [8, 9], as well as methods to mitigate them [10], yields clear routes towards sufficiently high current densities. The feasibility of Bi-2212 for accelerator magnets was recently demonstrated through Bi-2212 sub-scale coils that were fabricated and tested at LBNL [7], but reacted at the wire manufacturer. Here, we describe in detail the development of in-house coil reactions at LBNL, which are validated using the reaction and test of a new coil, HTS-SC10, using the same conductor and heat treatment as HTS-SC08, which was reacted at OST and tested at LBNL.

2. Furnace and calibrations

2.1. Furnace and instrumentation

One of the key issues with the reaction of Bi-2212 is the accurate control of the temperature, which becomes specifically difficult for larger structures such as insert coils. To allow for accurate temperature control, we purchased a custom-build Mellen Series SV11 Split Tubular furnace with a 324 mm bore, and 6 heating zones distributed over a 1016 mm heated zone. The 6 zones are computer controlled using type K thermocouples that are placed next to the heating elements, yielding a 610 mm homogeneous zone that is specified to be within ±1 °C. The furnace is equipped with an custom-build load-frame constructed of Alumina and INCONEL® 600. Type N thermocouples were used for the coil instrumentation (see Figure 1), which were manufacturer calibrated at 830 and 890 °C. The coil temperatures are recorded by NIST certified thermocouple loggers from OMEGA Engineering Inc.

2.2. Thermocouple calibrations

Though the thermocouples were manufacturer calibrated, the warranted accuracy is less than what is required for Bi-2212 reactions. The thermocouples were therefore mounted in an INCONEL® 600 isothermal block which was fully enclosed by an Ag dummy coil, and heated following a shortened reaction in flowing 100% Oxygen of 2 cubic feet per hour across the furnace volume of approximately 5 cubic feet. Deviations of about 2 – 3 °C were detected in the thermocouple readouts. Three runs were performed with the thermocouples in varying locations inside the isothermal block to distinguish between potential, but unlikely, temperature gradients across the isothermal block, and systematic errors in the thermocouple calibrations and readout. The systematic errors were then corrected for, and the resulting relative uncertainty in the temperature measurements of 12 type N thermocouples is shown in Figure 2 for the critical high temperature step in the reaction. The relative uncertainty across the thermocouple readouts in all three runs, with the

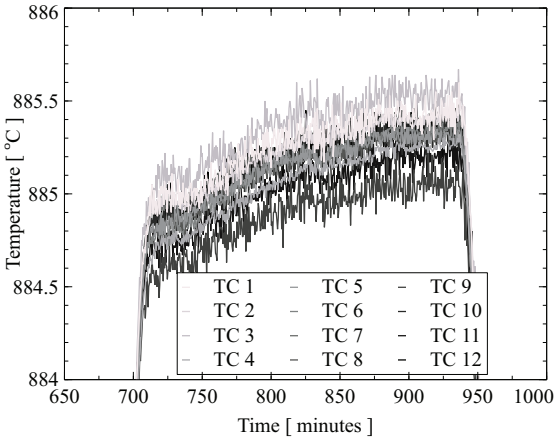

Fig. 2. Relative temperature uncertainty for 12 thermocouples mounted in an isothermal block.

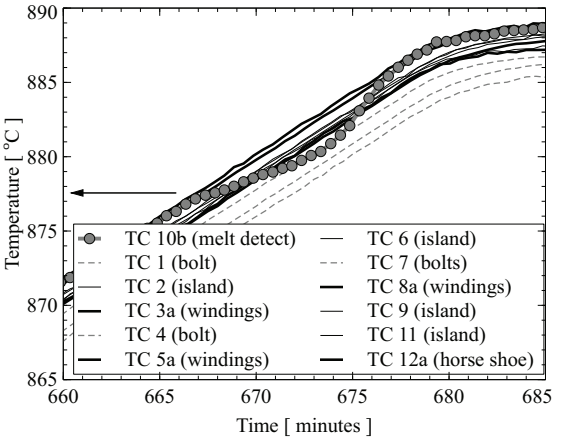

Fig. 3. Detection of the melting of Bi-2212 during a test reaction of an Ag dummy coil.

Table 1. Recorded T_{max} temperatures during the reaction of an Ag-dummy coil.

Region	Winding pack				Island				Bolts			
Thermocouple	8a	3a	12a	5a	9	2	6	11	10a	7	4	1
Temperature [°C]	888.7	888.7	889.2	888.0	888.2	888.2	888.0	888.0	885.0	886.4	886.3	885.7

thermocouples in varying locations inside the isothermal block, amounts to ±0.3 °C. The visible ramp in Figure 2, as well as the absolute temperature, were adjusted before the coil heat treatment.

A section of unreacted Bi-2212 wire was wrapped around the tip of a thermocouple and bolted to the dummy coil structure at position 10b in Figure 1. This thermocouple is used to detect the onset of melting of the Bi-2212 and thus provide an absolute temperature calibration [11]. The remaining thermocouples were placed in bolts (1, 2, and 7), the island (2, 6, 9, and 11) and inside the Ag dummy windings (3a, 5a, 8a, and 12a). The thermocouple response during the onramp towards the high temperature step in the reaction in 100% O_2 is shown in Figure 3. The melting of the Bi-2212 is clearly detected, and the onset of melting is, at about 877.5 °C, identical to the expected 878 °C within the accuracy by which the onset can be determined.

2.3. Coil temperature calibrations

The coil temperature homogeneity is investigated by analyzing the thermocouple responses during the reaction of an Ag dummy coil that is additionally equipped with twelve unreacted straight Bi-2212 wire sections. These wire sections were placed on pure SiO_2 braided tape on top of the Ag dummy coil in positions A – F in Figure 1. The ends of the wire sections were sealed by clamping Ag-foil around the wire ends. The dummy coil was reacted similar to coil HTS-SC08, and the I_c's of the wire sections were determined for a central 10 mm length of 50 mm samples at $E_c = 10^{-5}$ Vm^{-1}. The resulting temperature readouts at maximum temperature during the reaction and at the indicated positions across the Ag dummy coil are given in Table 1. The resulting I_c values for the straight wire sections are summarized in Table 2.

From Table 1 it is seen that the temperature of the windings is 888.6±0.6 °C, or 888.6±0.9 °C if the relative uncertainty of the thermocouple readout is added. It is also seen that the temperature of the island

Table 2. Self-field critical currents at $E_c = 10^{-5}$ Vm^{-1} of the straight wires sections that were reacted with the Ag-dummy coil.

Region	A	B	C	D	E	F
Sample 1 I_c [A]	384	375	—	388	319	343
Sample 2 I_c [A]	361	361	366	382	308	313

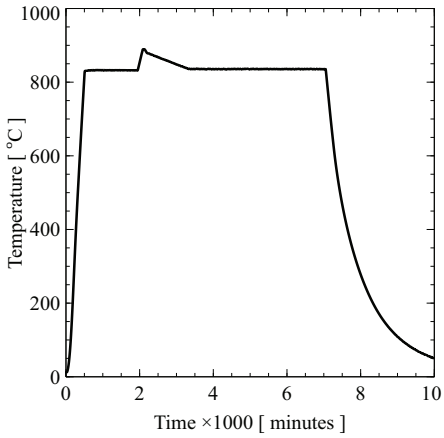

Fig. 4. Total recorded temperature as a function of time during the reaction of coil HTS-SC10.

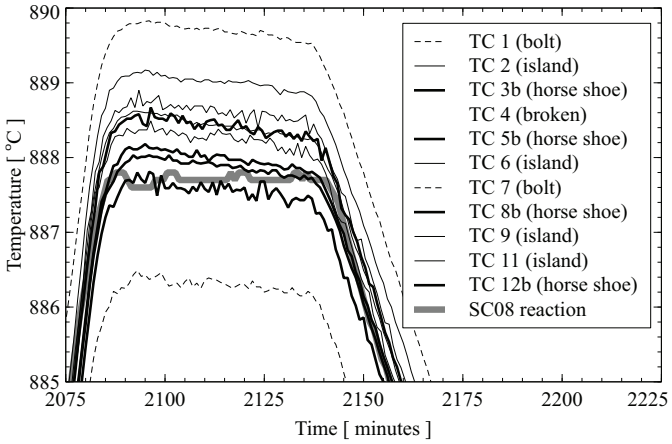

Fig. 5. High temperature detail of the temperature during the reaction of coil HTS-SC10.

is similar to the temperature of the windings, but that the bolts are 2 – 3 °C cooler than the central coil regions. The variation in the I_c values for the wire sections is inconsistent with the recorded temperature variations. A likely explanation of this is a difference in bubble density across the wire sections, caused by inconsistency in gas-tight sealing of the wire ends. Bubbles are formed by agglomeration of residual void fraction in the as-manufactured wires, outgassing of parasitic elements in the Bi-2212 powder, and release of O_2 during the melting of the Bi-2212 [8]. If wire ends are open, gas can escape from the ends and the bubble density will be reduced compared to fully sealed wire ends. This is similar to what was recently observed by Malagoli *et al.* [9], who compared sealed and unsealed wires and found a lower I_c and Bi-2212 density in the central regions of long unsealed samples. A measurement of the Bi-2212 density in the wire sections is planned to further investigate this possible cause for the variation in I_c for the short wire sections.

3. Reaction of HTS-SC10

Coil HTS-SC10 was reacted after having established that the temperature readouts and temperature homogeneity during the reaction are sufficiently accurate. Coil HTS-SC10 was reacted as similar as possible to the reaction of coil HTS-SC08 at OST. The recorded temperatures as a function of time are shown in Figure 4, and a magnification of the critical high temperature step is given in Figure 5. One of the thermocouple readouts from the reaction of coil HTS-SC08 is included in Figure 5. Two INCONEL® 600 helical sample holders with 1.2 m wire sections were reacted together with the coil.

It is seen that the island (thin lines) is on average about 0.5 °C warmer than the horse shoe (bold lines), suggesting a small temperature gradient from inside to outside. The windings are located between the island and the horse shoe and the winding temperature is therefore, taking into account this small gradient and the relative thermocouple uncertainty, within 888.4±1°C, whereas coil HTS-SC08 was reacted at 887.8±1°C [7]. Other factors, such as the local oxygen flow and concentration, might also differ slightly and could affect the coil performance. It is peculiar to observe that the bolt temperatures are not both lower than the central region of the coil, but that the TC7 temperature is higher. The reason for this is unclear.

4. Performance of coil HTS-SC10

After reaction, coil HTS-SC10 was prepared for measurement in a similar way to HTS-SC08 [7]. LBNL's superconducting transformer system [12] was used to provide the current during the coil I_c test at 4.2 K in self-field. Coil voltages were recorded while slowly ramping the current at -1.8 As^{-1}. The resulting electric field as a function of current for different coil sections and the total coil are given in Figure 6. The positions of the voltage taps with respect to the 2×6 coil turns are given in Figure 7.

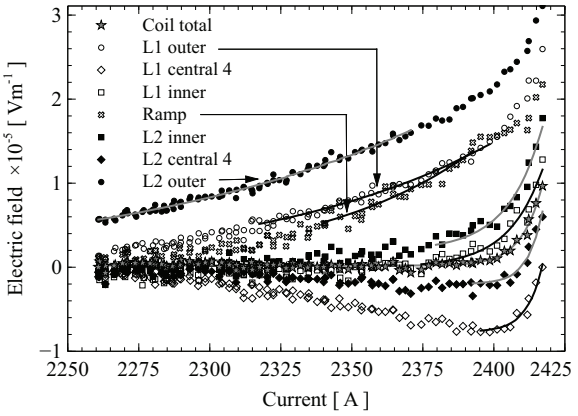

Fig. 6. Electric field as a function of current for the indicated sections of coil HTS-SC10 at 4.2 K in self-field.

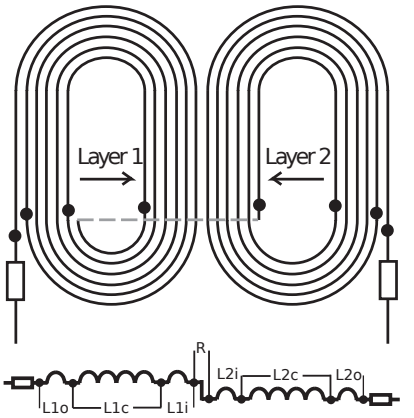

Fig. 7. Schematic representation of the voltage tap locations in coil HTS-SC10.

Table 3. Comparison of coil critical current values, determined at $E_c = 10^{-5}$ Vm^{-1}

	HTS-SC08	HTS-SC10
Total coil	2636 [a]	2417
L1 outer	2636 [a]	*2369*
L1 central	2636 [a]	2418
L1 inner	*2608*	2415
Ramp	*2589*	*2375*
L2 inner	*2557*	2412
L2 central	2636 [a]	2418
L2 outer	2636 [a]	*2319* [b]

[a] Quench value
[b] Includes short straight section to splice

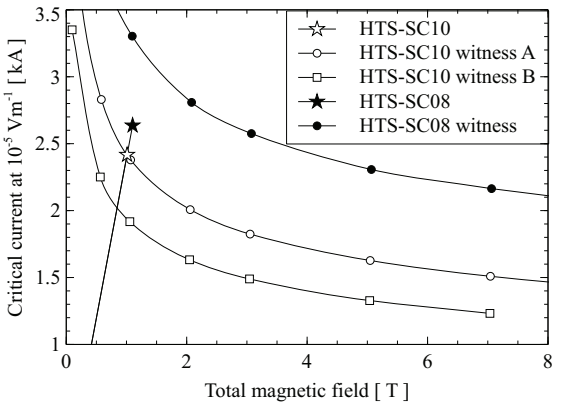

Fig. 8. Coil critical currents compared to the helical wires. The wire critical current values are multiplied by 17, the number of strands in the cable.

The largest voltages are generated by the ramp and the outer turns. The outer turn of layer 2 includes a short cable section next to a splice. It is therefore possible that some heating occurs for this section. Previous coils were, in contrast, limited by the inner turns and the ramp. The reason for this discrepancy is, for now, unclear. Negative voltages occur for the central regions. These are indicative for inhomogeneous current distributions with respect to the point from which the voltage taps pick up voltage. The determination of the I_c and n-values becomes somewhat subjective, as a result of these negative voltages. The $E(I)$ data are locally fitted to $E = E_0 + E_c(I/I_c)^n$ preferably around the E_c criterion, but this is not possible for all transitions. The lines in Figure 6 indicate across which data points the fit is made. The resulting I_c values are compared to those from coil HTS-SC08 in Table 3. The values in italic highlight the limiting sections. The helical witness samples were transferred to Ti-6Al-4V holders and measured up to 15 T. Comparisons of the coil performance to the helical witness samples is shown in Figure 8.

The performance of HTS-SC10 is within 10% of HTS-SC08 indicating a good reproducibility, specifically compared to the short sample sections that were reacted with the dummy coil. Redistribution of the current in the cable around local low I_c sections, which is more difficult in single wires, can be the reason for this higher reproducibility in the coils. The small difference between the coils can have various origins. Coil HTS-SC10 was held at 150 °C for 1.5 weeks to harden the epoxy as a result of an issue during impregnation, whereas coil HTS-SC08 was cured within a day. Further differences, such as the slightly higher temperature at which coil HTS-SC10 was reacted, or local oxygen concentration differences, are other possible causes.

Comparing the performance of HTS-SC10 with its helical witness wires (Figure 8) gives the impression that it reaches 100% of the current in the highest witness sample, compared to about 85% for coil HTS-SC08 (measured along the loadline). However, the I_c's of the helical witness wires differ significantly, at 248 and 197 A (4.2 K, self-field), and are substantially lower than the 308 – 388 A range that was observed in the short sections reacted with the dummy coil (Table 2). This raises the question whether the samples were damaged during transfer to the measurement holder, or whether intrinsic variations occur, similar to the short wire sections. More general, it raises the question what has to be considered the "short sample" value, which is commonly used to judge magnet performance. Here, the potential of wire is, at 388 A, substantially higher than the 248 A that was measured for the best helical witness wire.

5. Conclusions

It is shown that it is possible to react 30 cm long insert coils with a temperature accuracy of ±1 °C across the 2×6 turn winding pack. The performance of two identical coils, prepared in the same way, but reacted at two different institutes, reproduces within 10%, giving confidence in the reliability of the coil fabrication, reaction, and test procedures. The reproducibility of the coils is better than the reproducibility of helical witness samples, who's reproducibility is better than that of short straight wire sections. The likely cause for this is the increased influence of a local defect on the measured I_c when the sample becomes shorter, and the possibility for redistribution is reduced. The low reproducibility in shorter samples raises the question what has to be regarded as the "short sample" for HTS coil technology validation.

Acknowledgments

The authors would like to thank P. A. Bish, H.C. Higley, D. Horler, N. L. Liggins, J. Swanson, and P. Wong for their technical assistance, and OST for providing the thermocouple data for the reaction of coil HTS-SC08. This work was supported by the Director, Office of Science, High Energy Physics, U.S. Department of Energy under contract No. DE-AC02-05CH11231.

References

[1] A. Godeke, D. Cheng, D. R. Dietderich, P. Ferracin, S. O. Prestemon, G. Sabbi, R. M. Scanlan, Limits of NbTi and Nb_3Sn, and development of W&R Bi–2212 high field accelerator magnets, IEEE Trans. Appl. Supercond. 17 (2) (2007) 1149.

[2] A. F. Lietzke, S. Bartlett, P. Bish, S. Caspi, L. Chiesa, D. Dietderich, P. Ferracin, S. A. Gourlay, M. Goli, R. R. Hafalia, H. Higley, R. Hannaford, W. Lau, N. Liggens, S. Mattafirri, A. McInturff, M. Nyman, G. Sabbi, R. Scanlan, J. Swanson, Test results for HD1, a 16 Tesla Nb_3Sn dipole magnet, IEEE Trans. Appl. Supercond. 14 (2) (2004) 345–348.

[3] D. R. Dietderich, M. Kelman, J. R. Litty, R. M. Scanlan, High critical current densities in Nb_3Sn films with engineered microstructures – artificial pinning microstructures, Adv. Cryo. Eng. (Materials) 44B (1998) 951–959.

[4] D. R. Dietderich, A. Godeke, Nb_3Sn research and development in the USA - Wires and cables, Cryogenics 48 (2008) 331.

[5] C. A. Rodrigues, D. Rodrigues Jr., Flux pinning behavior of Nb_3Sn superconductors with nanostructured pinning centers, IEEE Trans. Appl. Supercond. 17 (2) (2007) 2627–2630.

[6] D. Rodrigues Jr., L. B. S. Da Silva, C. A. Rodrigues, N. F. Oliveira Jr., C. Bormio-Nunes, Opimization of heat treatment profiles applied to nanometric-scale Nb_3Sn wires with Cu-Sn artificial pinning centers, IEEE Trans. Appl. Supercond. 21 (3) (2011) 3150–3153.

[7] A. Godeke, P. Acosta, D. Cheng, D. R. Diederich, M. G. T. Mentink, S. O. Prestemon, G. L. Sabbi, M. Meinesz, S. Hong, Y. Huang, J. Parrell, Wind-and-react Bi-2212 coil development for accelerator magnets, Supercond. Sci. and Techn. 23 (2010) 034022 (6pp).

[8] F. Kametani, T. Shen, J. Jiang, C. Scheuerlein, A. Malagoli, M. D. Michiel, Y. Huang, H. Miao, J. A. Parrell, E. E. Hellstrom, D. C. Larbalestier, Bubble formation within filaments of melt-processed Bi2212 wires and its strongly negative effect on the critical current density, Supercond. Sci. and Techn. 24 (7) (2011) 075009.

[9] A. Malagoli, F. Kametani, J. Jiang, U. P. Trociewitz, E. E. Hellstrom, D. C. Larbalestier, Evidence for long range movement of Bi-2212 within the filament bundle on melting and its significant effect on J_c, Supercond. Sci. and Techn. 24 (7) (2011) 075016.

[10] J. Jiang, W. L. Starch, M. Hannion, F. Kametani, U. P. Trociewitz, E. E. Hellstrom, D. C. Larbalestier, Doubled critical current density in Bi-2212 round wires by reduction of the residual bubble density, Supercond. Sci. and Techn. 24 (8) (2011) 082001.

[11] A. Tollestrup, Temperature profile measurements during heat treatment of BSCCO 2212 coils, Technical Report Fermilab-tm-2505-apc, Fermilab (2011).

[12] A. Godeke, D. R. Diederich, J. M. Joseph, J. Lizarazo, S. O. Prestemon, G. Miller, H. W. Weijers, A superconducting transformer system for high current cable testing, Rev. Sci. Instr. 81 (2010) 035107 (9 pp).